Effects of pile length on the settlement behavior of floating energy piles subjected to thermal cycles

Charles W. W. Ng & Q. J. Ma
Department of Civil and Environmental Engineering – Hong Kong University of Science and Technology, Hong Kong, China

ABSTRACT
Centrifuge modelling of floating energy piles subjected to cyclic thermal loading was conducted in saturated Toyoura sand, with focus on the effects of the embedded pile length. The energy piles were applied 15 two-way heating-cooling cycles with an amplitude of about 10 °C. A constant vertical working load with a factor of safety equal to 2.0 was maintained during the test. Reference piles with the same working load but not cyclic thermal loading were also tested for comparison. The results show that the energy piles experience ratcheting settlement during thermal cycles, and accumulate more irreversible settlement compared to the reference piles. The irreversible settlement of the energy piles tends to stabilize with thermal cycles, but does not stabilize completely by the end of the 15 thermal cycles. In addition, it is observed that as the embedded pile length increases the accumulated irreversible settlement of energy piles decreases.

RÉSUMÉ
La modélisation par centrifugation de pieux énergétiques flottants soumis à un chargement thermique cyclique a été réalisée dans du sable saturé de Toyoura, en mettant l'accent sur les effets de la longueur de la pile enfouie. Quinze cycles de chauffage et de refroidissement bidirectionnels d'une amplitude d'environ 10 °C ont été appliquées aux pieux énergétiques.Une charge de travail verticale constante avec un facteur de sécurité égal à 2,0 a été maintenue pendant l'essai. Les pieux de référence ayant la même charge de travail mais non la charge thermique cyclique ont également été testés pour comparaison. Les résultats montrent que les pieux énergétiques subissent un tassement à cliquet au cours des cycles thermiques et accumulent un tassement plus irréversible par rapport aux pieux de référence. Le tassement irréversible des pieux énergétiques tend à se stabiliser avec les cycles thermiques, mais ne se stabilise pas complètement à la fin des 15 cycles thermiques. De plus, on observe que lorsque la longueur de la pieux enfoncée augmente, le tassement accumulé irréversible des pieux énergétiques diminue.

1 INTRODUCTION

Experimental study (e.g. Kalantidou et al., 2012; Ng et al., 2016a; Nguyen et al., 2017) reveals that when subjected to cyclic thermal loading single floating energy piles show a ratcheting settlement behavior, gradual accumulation of irreversible settlement at a reducing rate as demonstrated in Fig. 1. For end-bearing conditions, the pile settlement behavior under thermal cycles is almost reversible (Stewart & McCartney, 2013). Ng et al. (2016b) tried to explore the reason behind this phenomenon by finite element modelling, and significant reduction of horizontal stress is noticed from the numerical simulation. This study aims to further the research to investigate the effects of the embedded pile length on the settlement behavior of floating energy piles subjected to cyclic thermal loading via centrifuge modelling. In addition, the finite element model developed by Ng et al. (2016b) was also examined via back-analyzing the centrifuge tests.

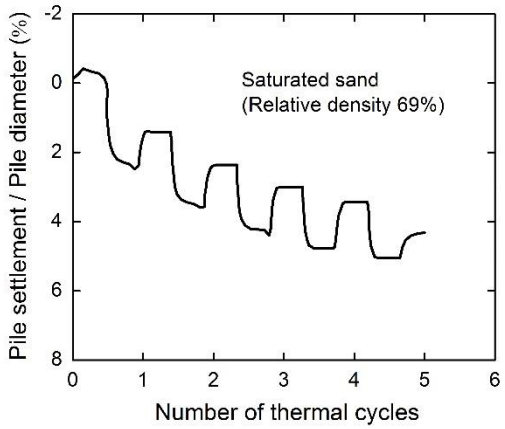

Figure 1. Ratcheting settlement behavior of single floating energy piles subjected to cyclic thermal loading in sand (reproduced from Ng et al., 2016a)

2 CENTRIFUGE MODELLING

The centrifuge tests reported in this study were carried out at the Hong Kong University of Science and Technology (HKUST) at the target g-level of 60g. All the dimensions used below are in the model scale. The scaling laws listed in Table 1 can be tentatively used to extrapolate the test results to the prototype scale.

2.1 Model soil and model pile

In this study Toyoura sand was used, the basic properties of which are listed in Table 2. The Toyoura sand has a critical state friction angle of 31°, with the mean particle size d_{50} of 0.17 mm. Its minimum and maximum void ratio

are 0.597 and 0.977, respectively. The sand layer was prepared by air raining from a constant falling height of 1 m to the soil surface. The average relative density achieved was about 65 ± 2%.

Steel pipes with a hollow square cross section to allow for the water circulation were adopted as model piles. The steel material had a similar coefficient of linear thermal expansion to that of concrete (1.2×10^{-5} against about 1.0×10^{-5}). The outside cross section dimension of the model pile was 19 × 1.6 mm. Three thermocouples evenly distributed along the pile length were installed on it to monitor its temperature change. The model piles were covered by a 1.5 mm thick epoxy layer to protect the thermocouples. The resultant pile width B was 23 mm. The ratio of B / d_{50} was about 135, larger than 100. The particle size effects was thus expected to be negligible according to Garnier et al. (2007). The total self-weight of each model pile was 990 g.

Table 1. Scaling laws (Garnier et al., 2007)

Parameter	Model	Prototype
Gravitational acceleration	N	1
Length	1	N
Displacement	1	N
Density	1	1
Stress	1	1
Strain	1	1
Temperature	1	1
Time (diffusion)	1	N^2

[1]N is the target g-level.

Table 2. Basic properties of Toyoura sand (Ishihara, 1993)

Property	Value
Critical state friction angle, φ	31°
Mean particle size, d_{50}	0.17 mm
Minimum void ratio, e_{min}	0.597
Maximum void ratio, e_{max}	0.977
Specific gravity, G_s	2.65

2.2 Test Setup

The centrifuge test setup is schematically shown in Fig. 2 schematically. A total of four floating piles, two reference piles and two energy piles, were put in the same model box with the size of 1245 x 350 x 850 mm. The thickness of the sand layer was 750 mm. The embedded length of the long piles and the short piles was 550 mm and 250 mm, respectively. To maximize the separation, the four piles were located uniformly along the longitudinal direction with a clear distance between them around 230 mm (10B). Therefore, the pile-pile interaction was considered to be negligible (O'Neill, 1983). The nearest distance from the wall to the pile was 175 mm, slightly less than 8B. According to Bolton et al. (1999), no significant boundary effects were expected. Vertically, the pile base was 200 mm above the bottom of the model box for the long piles, and 500 mm for the short piles.

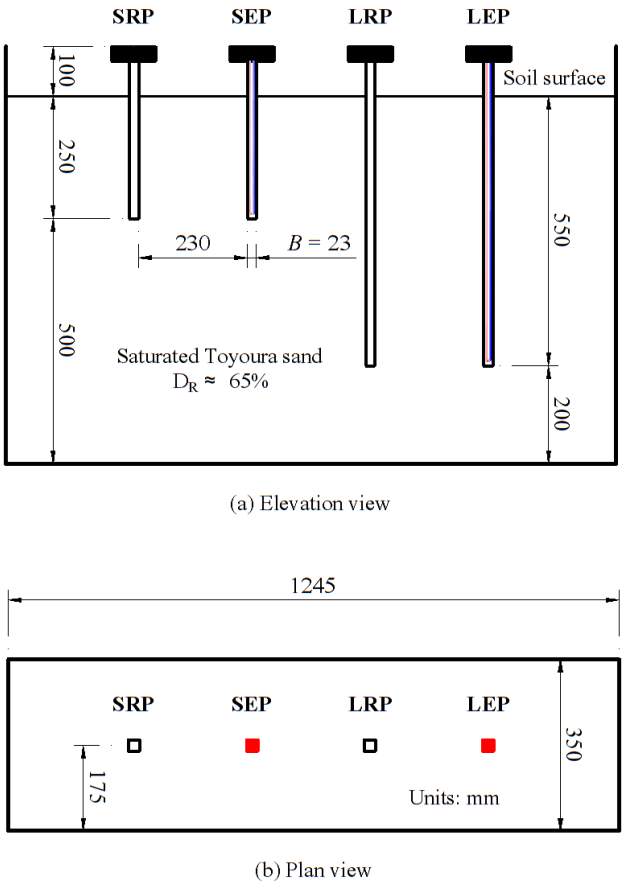

Figure 2. Schematic diagram of test setup: (a) elevation view; (b) plan view. (SRP, SEP, LRP and LEP stand for short reference pile, short energy pile, long reference pile and long energy pile, respectively)

2.3 Test Procedure

Before increasing the g-level to 60g, the sand layer was naturally submerged under water to increase its thermal conductivity. The thermal conductivity of soils increases with the water content according to Brandl (2006). The dead weight was fixed rigidly on top of the piles to simulate the constant vertical working load under the target g-level. The working load was determined based on independent pile failure loading tests. The failure criterion proposed by Ng et al. (2001) was used to estimate the pile bearing capacity. Adopting a factor of safety equal to 2.0, the corresponding working load for the long pile and the short pile was determined to be 660 N and 180 N, respectively. Linear variable differential transformers (LVDTs) were attached on top of the dead weight to monitor the pile head displacement. After spinning-up, about 3 hours were waited for equilibrium before application of 15 heating-

cooling cycles on the two energy piles. Each heating or cooling phase was 48 mins. Another 3 hours were waited before spinning down, referred to as the recovery stage. The test procedure is illustrated in Fig. 3. The long energy pile and the short energy pile were connected in parallel, and heated or cooled simultaneously. In this way they were supposed to experience the same temperature change, ensuring a valid comparison between them. The heating or cooling of the pile body was achieved by circulating the temperature-controlled water through the pile body. The circulating water went through a heating-cooling system to reach the target temperature. The heating-cooling system was mounted on top of the centrifuge, and the circulation pipes went down to the platform. For more details on the heating-cooling system, please refer to Ng et al. (2016a).

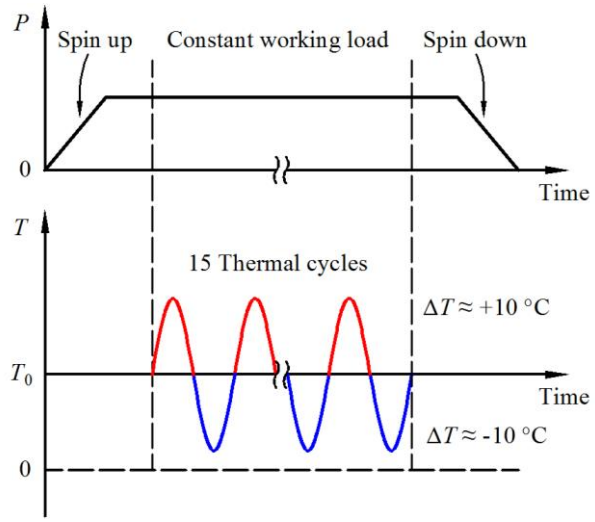

Figure 3. Illustration of the test procedure (*P* and *T* stand for vertical working load and temperature, respectively)

3 NUMERICAL MODELLING

The axi-symmetric finite element model developed by Ng et al. (2016b) was also used to simulate the effects of the embedded pile length on the settlement behavior of floating energy piles subjected to cyclic thermal loading. The commercial software Abaqus was used.

The numerical analysis only considers the mechanical aspect of the energy pile-soil interaction problem without simulating the heat transfer process through the soil. The energy pile itself was assumed to behave thermo-elastically. As a result, the repeated thermal expansion and contraction of the pile body resulting from the thermal cycles exerts cyclic shearing on the surrounding soil. To properly consider the potential volume change induced by the cyclic shearing, the state-dependent dilatancy should be well simulated. Therefore, the incrementally nonlinear Hypoplastic model developed by Niemunis and Herle (1997) was adopted for the sand model. Niemunis & Herle extended von Wolffersdorff's model (1996) by introducing the concept of inter-granular strain to improve the simulation of soil behavior under cyclic loading. The concept of inter-granular strain represents essentially a small elastic range, and also enables the proper consideration of the effects of recent stress history. It should be noted that the adopted Hypoplastic soil constitutive model cannot consider the possible thermal effects on soil. The thermal effects on sand is relatively small, and mainly presents itself within the first thermal cycle (Ng et al., 2016c). Therefore, the adoption of the Hypoplastic constitutive model for this study is justified despite its incapability of modelling thermal effects. The pile-soil interaction is modelled using the basic Coulomb frictional model.

A typical finite element mesh is shown in Fig. 4. Bilinear elements were adopted with the aspect ratio of mesh elements around 1.0. As can be seen from the figure, the regions adjacent to the pile body and below the pile base were particularly refined in order to capture the possible nonlinear soil response surrounding the pile. The vertical displacements on bottom of the model and the horizontal displacements on two sides of the model were constrained. To simulate the square energy pile using this axi-symmetric finite element model, the pile diameter *D* was taken to be the same as the pile width *B*. The major intention here is to examine the capability of the finite element analysis in a qualitative sense. For more details on the numerical modelling, please refer to Ng et al. (2016b).

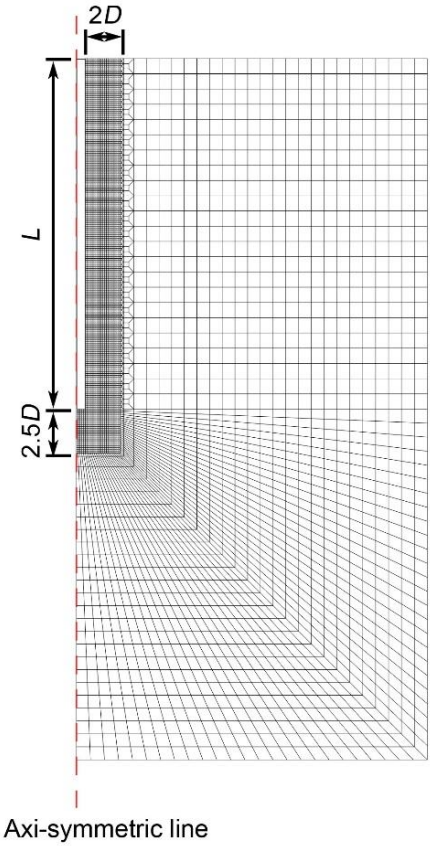

Figure 4. Typical finite element mesh (*D* and *L* stand for pile diameter and embedded pile length, respectively)

4 RESULTS

All the test results are reported in the model scale.

4.1 Temperature

Figure 5 shows the measured temperature variation of the long energy pile during thermal cycles from the three thermocouples (TC) installed on it. Also included in the figure is the ambient temperature. The ambient temperature is necessary for the interpretation of the thermocouple results. The thermocouple only measures the temperature difference between the monitored point and the reference point which corresponds to the ambient. The results show that the three monitored points (TC – Top, TC – Middle and TC - Bottom) of the long energy pile experience almost the same temperature change, with an amplitude slightly larger than 10 °C. Closer observation reveals that the temperature change of the three monitored points decreases slightly from the pile toe to the pile head. This is because of two reasons. The circulating fluid goes down to the bottom of the pile body directly through a pipe inserted inside the pile body, and then flows upwards to heat or cool the pile body. During the process of flowing upwards, there is some heat loss. Thus the bottom point experiences the highest temperature change. In addition, the ambient air with a relatively constant temperature behaves as a heat sink. Therefore the heat transfer between the soil surface and the air can have some effects on the temperature change of the top point.

Each heating or cooling phase lasted for 48 mins. During this period, there occurs some heat transfer through the soil. As a consequence, the temperature of the soil can also be changed as shown in Fig. 6 for the long energy pile. The two monitored points of the soil temperature change were located 0.5*B* and 1.5*B* to the pile surface, respectively. In the vertical direction, both of them were on the same horizontal plane halfway the embedded pile length. The soil temperature change follows the overall trend that the farther away from the energy pile the less temperature variation. The amplitude of the temperature variation is about 6 °C and 4 °C for the two points located 0.5*B* and 1.5*B* to the pile surface, respectively. A similar pattern is observed for the case of the short energy pile.

Figure 7 compares the monitored temperature change of the long energy pile and the short energy pile. The average temperature change calculated from the three thermocouples is shown in this figure. It demonstrates that there is almost no difference in temperature change between the long energy pile and the short energy pile. This is due to the fact that the long energy pile and the short energy pile were connected in parallel, and the circulating fluid went through them simultaneously. It should be mentioned that the target temperature of the circulating fluid leaving the heating-cooling system was controlled in the centrifuge test. During the process of flowing downwards from the top of the centrifuge to the platform, inevitably there was some heat transfer between the circulating fluid and the environment. Consequently, the slightly varying ambient temperature as shown in the figure can have some effects on the temperature change experienced by the energy piles. This is why the measured amplitude of temperature change of the energy piles shows some slight variation as the cyclic thermal loading continues. Overall, a relatively constant amplitude of temperature change about 10 °C was achieved for the two energy piles tested.

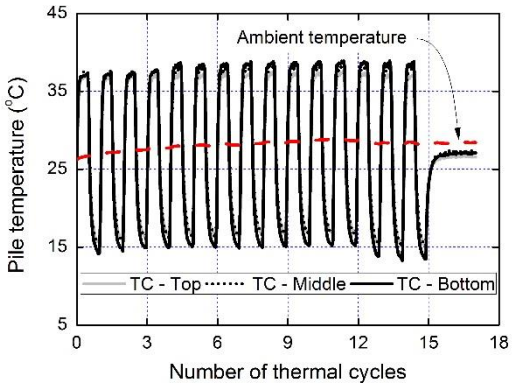

Figure 5. Temperature variation of the long energy pile during thermal cycles (TC stands for thermocouple)

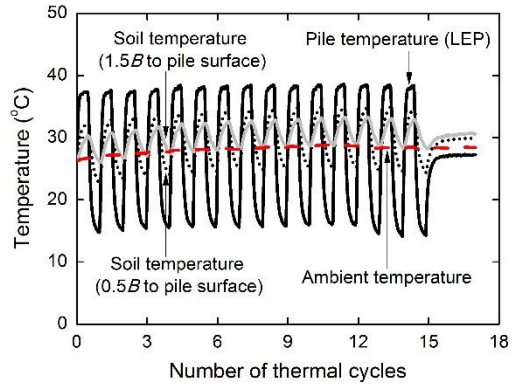

Figure 6. Temperature variation of the soil adjacent to the long energy pile during thermal cycles

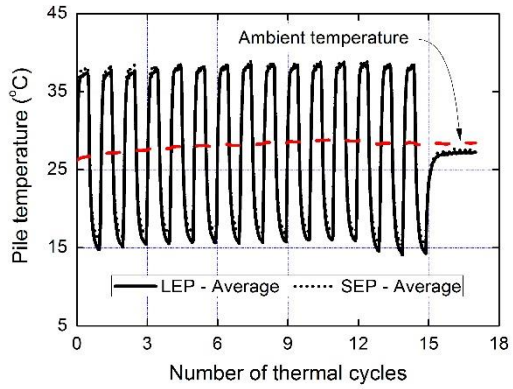

Figure 7. Comparison of temperature variation of the long energy pile and the short energy pile during thermal cycles

4.2 Displacement from centrifuge modelling

Figure 8 shows the measured pile head displacement of the energy piles together with the reference piles during the thermal cycles and the following recovery stage. The pile head displacement is normalized against the pile width (B = 23 mm). It can be seen that the two reference piles show a continuous creep settlement with the difference between them almost negligible. This is because the pile creep settlement is governed by the working load level, and the same factor of safety equal to 2.0 was adopted for all the piles tested in this study.

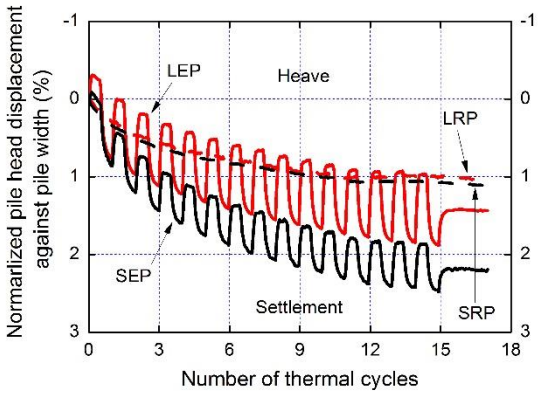

Figure 8. Pile head displacement during thermal cycles from centrifuge modelling (SRP, SEP, LRP and LEP stand for short reference pile, short energy pile, long reference pile and long energy pile, respectively)

Differing from the reference piles, the energy piles show a ratchetting settlement behavior. The energy piles heave during heating (vertical elongation) and settle during cooling (vertical shortening). Overall, there is some accumulation of irreversible settlement as the cyclic thermal loading continues, but at a reducing rate. This pattern is similar to previously reported test results as shown in Fig.1. It should be noted that the irreversible settlement of energy piles tends to stabilize, but does not stabilize completely after 15 two-way thermal cycles with an amplitude of about 10 °C. During the following recovery stage, the settlement of the energy piles is almost the same as that of the reference piles, and only some slight settlement is observed. Compared to the reference piles, cyclic thermal loading induces some additional irreversible pile settlement. This additional irreversible pile settlement is more significant for the short energy pile than for the long energy pile. It is about 1.1% B for the short energy pile against roughly 0.5% B for the long energy pile by the end of the recovery stage. This observed trend is just opposite to the suggested increase of additional irreversible pile settlement with the pile length by the Ground Source Heat Pump Association (2012). In addition, the accumulated irreversible settlement by the end of the recovery stage is less than the reference value of about 3.6% B (50 mm in prototype) as suggested by the Eurocode 7 (2004) for the serviceability limit state.

4.3 Displacement from numerical modelling

Three cases with different embedded pile lengths (250 mm, 400 mm and 550 mm) were simulated using the finite element model. The cases with the embedded pile length of 250 mm and 550 mm were the back-analysis of the short energy pile and the long energy pile of the centrifuge test, respectively. The case with the embedded pile length of 400 mm was to confirm the overall trend. The obtained variation of pile head displacement with thermal cycles for the three cases simulated is shown in Fig. 9. It can be seen that the numerical analysis also gives a ratcheting settlement behavior for all the three cases. However, just contrary to the experimental results, the numerical results show that as the embedded pile length increases the pile experiences more irreversible ratcheting settlement. It is known that for floating piles the ratio of mobilized shaft resistance to mobilized base resistance under working load increases with the embedded pile length. According to Ng et al. (2016b), under cyclic thermal loading floating energy piles experience a significant loss of horizontal stress. Therefore, the numerical analysis predicts more settlement for the long energy piles to mobilize more base resistance compensating for the reduction of the shaft resistance. The contradiction in settlement behavior between the experimental results and the numerical results necessitates further experimental work to measure the horizontal stress change of floating energy piles subjected to cyclic thermal loading.

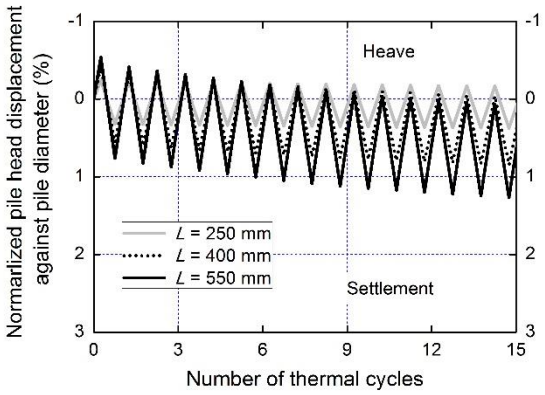

Figure 9. Pile head displacement during thermal cycles from numerical modelling (L stands for embedded pile length)

5 CONCLUSIONS

This paper reports a centrifuge study to investigate the effects of the embedded pile length on the settlement behavior of floating energy piles subjected to cyclic thermal loading. Numerical modelling was also performed and compared to the experimental results. Based on the results and comparison presented above, the authors attempt to draw the following conclusions:

When subjected to cyclic thermal loading, floating energy piles experience some ratchetting settlement,

which does not stabilize after 15 thermal cycles with an amplitude of about 10 °C. Relative to the reference piles, cyclic thermal loading induces some additional irreversible pile settlement, which decreases as the embedded pile length increases.

Compared to the experimental results, the numerical results show a contradictory trend regarding the effects of the embedded pile length. This is possibly due to the over-prediction of the horizontal stress reduction with thermal cycles. As shown in Ng et al. (2016b), the horizontal stress reduction may reach up to 90%. Further experimental work is necessary to verify the significant loss of horizontal stress for floating energy piles under thermal cycles as predicted by the numerical analysis.

6 ACKNOWLEDGEMENTS

The second author greatly appreciates the HKPFS scholarship offered by the Research Grants Council (RGC) of the HKSAR. The financial support provided by the RGC of the HKSAR (grant no. GRF 617213 and 16209415), the HKUST (grant no. FP204) and the National Science Foundation of China (grant no. 51378178) are also gratefully acknowledged.

7 NOTATION

B	Pile width
D	Pile diameter
L	Pile length
N	Target g-level
P	Pile head working load
T	Temperature
T_0	Initial temperature
ΔT	Change of temperature
φ	Critical state friction angle
d_{50}	Mean particle size
e_{min}	Minimum void ratio
e_{max}	Maximum void ratio
G_s	Specific gravity

8 REFERENCES

Bolton, M. D., Gui, M. W., Garnier, J., Corte, J. F., Bagge, G., Laue, J., & Renzi, R. (1999). Centrifuge cone penetration tests in sand. Géotechnique, 49(4), 543-552.

Brandl, H. (2006). Energy foundations and other thermo-active ground structures. Geotechnique, 56(2), 81-122.

BS EN 1997-1. (2004). Geotechnical design Part 1: General rules. Eurocode 7, 1(2004).

Garnier, J., Gaudin, C., Springman, S. M., Culligan, P. J., Goodings, D., Konig, D., & Thorel, L. (2007). Catalogue of scaling laws and similitude questions in geotechnical centrifuge modelling. International Journal of Physical Modelling in Geotechnics, 7(3), 1-23.

Ground Source Heat Pump Association. (2012). Thermal pile; design, installation & materials standards. Ground Source Heat Pump Association, Milton Keynes.

Ishihara, K. (1993). Liquefaction and flow failure during earthquakes. Geotechnique, 43(3), 351-451.

Kalantidou, A., Tang, A. M., Pereira, J. M. and Hassen, G. Preliminary study on the mechanical behaviour of heat exchanger pile in physical model. Géotechnique 2012; 62(11): 1047–1051.

Ng, C. W. W., Gunawan, A., Shi, C., Ma, Q. J. and Liu, H. L. (2016a). Centrifuge Modelling of Energy Pile – Comparative Performance: Displacement versus Replacement. Géotechnique Letters, 6(1): 1-5.

Ng, C. W. W., Ma, Q. J., & Gunawan, A. (2016b). Horizontal stress change of energy piles subjected to thermal cycles in sand. Computers and Geotechnics, 78, 54-61.

Ng, C. W. W., Wang, S. H., & Zhou, C. (2016c). Volume change behaviour of saturated sand under thermal cycles. Géotechnique Letters, 6(2), 124-131.

Ng, C. W. W., Yau, T. L., Li, J. H. & Tang, W. H. (2001). New failure load criterion for large diameter bored piles in weathered geomaterials. Journal of Geotechnical and Geoenvironmental Engineering, 127(6): 488–498.

Nguyen, V. T., Tang, A. M., & Pereira, J. M. (2017). Long-term thermo-mechanical behavior of energy pile in dry sand. Acta Geotechnica, 1-9.

Niemunis, A. and Herle, I. Hypoplastic model for cohesionless soils with elastic strain range. Mech. Cohes.-Frict. Mater. 1997; 2(4): 279-299.

O'Neill, M. W. (1983). Group action in offshore piles. In Proceedings of the Conference on Geotechnical Practice in Offshore Engineering, Austin, 25-64.

Stewart, M. A., & McCartney, J. S. (2013). Centrifuge modeling of soil-structure interaction in energy foundations. Journal of Geotechnical and Geoenvironmental Engineering, 140(4), 04013044.

von Wolffersdorff, P. A. A hypoplastic relation for granular materials with a predefined limit state surface. Mech. Cohes.-Frict. Mater. 1996; 1(3): 251-271.